Notch pathway inhibition targets chemoresistant insulinoma cancer stem cells

Accepted Preprint first posted on 24 November 2017 as Manuscript ERC-17-0415

Notch pathway inhibition targets chemoresistant insulinoma cancer stem cells

Capodanno Y[1 *], Buishand FO[2,*], Pang LY[1], Kirpensteijn J[3], Mol JA[2], Argyle DJ[1]

[1] Royal (Dick) School of Veterinary Studies and The Roslin Institute, University of Edinburgh, EH25 9RG, United Kingdom.

[2] Department of Clinical Sciences of Companion Animals, Faculty of Veterinary Medicine, Utrecht University, Utrecht, The Netherlands.

[3] Hill's Pet Nutrition, 400 W 8th Ave, Topeka, KS 66047, USA

[*] These authors contributed equally

Corresponding author: Ylenia Capodanno, Royal (Dick) School of Veterinary Studies and The Roslin Institute, University of Edinburgh, Easter Bush, EH25 9RG, United Kingdom, ylenia.capodanno@roslin.ed.ac.uk

Short title: Insulinoma cancer stem cells targeted therapy

Key words: NOTCH2; HES1; 5-fluorouracil; comparative oncology; endocrine pancreatic tumours

Word count: 4.983

Abstract

Insulinomas (INS) are the most common neuroendocrine pancreatic tumours in humans and dogs. The long-term prognosis for malignant INS is still poor due to a low success rate of the current treatment modalities, particularly chemotherapy. A better understanding of the molecular processes underlying the development and progression of INS is required to develop novel targeted therapies. Cancer stem cells (CSCs) are thought to be critical for the engraftment and chemoresistance of many tumours, including INS. This study was aimed to characterise and target INS CSCs in order to develop novel targeted therapies.

Highly invasive and tumourigenic human and canine INS CSC-like cells were successfully isolated. These cells expressed stem cell markers (*OCT4*, *SOX9, SOX2, CD133 and CD34*), exhibited greater resistance to 5-fluorouracil (5-FU), and demonstrated a more invasive and tumourigenic phenotype *in vivo* compared to bulk INS cells. Here, we demonstrated that Notch-signalling-related genes (*NOTCH2* and *HES1)* were overexpressed in INS CSC-like cells. Protein analysis showed an active NOTCH2-HES1 signalling in INS cell lines, especially in cells resistant to 5-FU. Inhibition of the Notch pathway, using a gamma secretase inhibitor (GSI), enhanced the sensitivity of INS CSC-like cells to 5-FU. When used in combination GSI and 5-FU, the clonogenicity *in vitro* and the tumourigenicity *in vivo* of INS CSC-like cells were significantly reduced. These findings suggested that the combined strategy of Notch signalling inhibition and 5-FU synergistically attenuated enriched INS CSC populations, providing a rationale for future therapeutic exploitation.

Introduction

Insulinomas (INS) are the most common functioning neuroendocrine pancreatic tumours (PancNETs) in humans and dogs. INS are insulin-producing tumours that arise from beta-cells (Wang *et al*. 2004; Bailey *et al*. 2007; Polton *et al*. 2007; Athanasopoulos *et al.* 2011; Baudin *et al*. 2014; Buishand *et al.* 2014). The treatment of choice for localised benign INS is surgical resection (Bailey *et al.* 2007; Buishand *et al.* 2014). However, for advanced stage disease medical treatment options for adjuvant therapy are limited. Combinations of chemotherapies such as streptozocin plus 5-fluorouracil (5-FU) or doxorubicin have been used in these cases, but response rates, are variable and generally disappointing (Corroller *et al.* 2008; Mathur *et al.* 2012). Thus, effective new treatment strategies are required.

We hypothesise that the malignant behaviour and recurrence of INS is driven by a subpopulation of cancer stem cells (CSCs). CSCs are unique subpopulations of the heterogeneous cell population of a tumour, which are considered to be responsible for tumour initiation, metastasis, and recurrence (Mitra *et al*. 2015). CSCs have been described to be able to resist systemic anti-cancer treatment by several mechanisms including entering into a quiescence state; up-regulation of expression of xenobiotic efflux pumps; and enhancing anti-apoptotic and DNA repair pathways to allow cell survival (Bomken *et al.* 2010). Therefore, CSCs are able to survive and initiate tumour relapse after systemic treatment, making them an essential target for novel anti-cancer drugs.

Despite the growing evidence to support the existence of CSCs in a wide array of solid tumours, a comprehensive characterisation of INS CSCs has not yet been reported (Grande *et al.* 2011). Previous studies have already identified pancreatic cells with a stem cell phenotype in human and canine INS (Ordonez, 2001; Buishand *et al*. 2013). These so-called amphicrine cells co-express both endocrine and exocrine markers (Ordonez, 2001).

Furthermore, recent studies have identified CD90 as a potential marker for CSCs in a human INS cell line (Buishand *et al*. 2016). However, there are no consensus markers available to identify INS CSC-like cells and additionally, recent studies show that several CSC populations may reside within one tumour (Hou *et al.* 2014; Krampitz *et al.* 2016).

The lack of knowledge regarding CSCs in INS can be partly attributed to the low incidence of human INS. With only four cases per million population per year, the availability of research material is limited, especially for malignant subtypes (Callacondo *et al.* 2013). Previously, investigators have analysed changes in gene expression of malignant INS mainly as part of broad studies on PancNETs (Speel *et al*. 1999; Zhao *et al*. 2001). However, PancNETs represent a heterogeneous group of tumours and therefore, the specific tumourigenesis of INS is still poorly understood. The incidence of canine INS has not been specified yet but it is higher compared to humans. Data collected at the Department of Clinical Sciences of Companion Animals of Utrecht University have recorded 10 referral cases of malignant canine INS on a yearly basis, out of a total of two million dogs in The Netherlands (FO Buishand, unpublished observations). This provides readily available canine INS samples for molecular studies.

Canine INS are classified as malignant tumours in 95% of the cases as they often metastasise to abdominal lymph nodes and liver (Buishand *et al.* 2010). As in humans, canine patients diagnosed with malignant INS are often presented with relapse of hyperinsulinaemia due to the outgrowth of micrometastases that were not detected at the time of initial surgery (Jonkers *et al.* 2007; Goutal *et al.* 2012). From a comparative oncology perspective, which aims to utilise spontaneous tumours in pet animals as natural models for the study of human cancer biology and therapy (Gordon *et al.* 2009), the close resemblance of canine INS to human malignant INS, makes canine INS an interesting study model for human malignant INS. The major benefit of comparing human INS cells to canine INS cells

instead of murine cells from genetically-induced INS mouse models (Schiffman *et al*. 2015) is that spontaneous canine tumour cells are more representative of the complex heterogeneity of INS, as they are not induced by a set of specific mutations, but arise spontaneously in a dog. Therefore, the translational gap between pre-clinical *in vitro* studies and the application of novel drugs in a clinical setting can be overcome by using naturally occurring canine INS as model for human INS (Gordon *et al.* 2009).

Using a comparative oncology approach, the first goal of this study was to isolate and characterise human and canine enriched INS CSC populations. As CSCs are known to often co-opt stem and progenitor cell properties, we have used the potential functional conservation of stem cell-surface and intrinsic enzymatic markers found on self-renewing cells to identify and characterise tumourigenic cells. We then set out to identify therapeutic targets in signalling pathways in INS, performing gene expression profiling of adherent INS cells and CSC-enriched tumourspheres. We showed that the Notch pathway is a critical pathway involved in INS CSC viability. Using both *in vitro* and *in vivo* models, we have demonstrated the efficacy of targeting the Notch pathway in decreasing INS CSC survival and resistance to 5-FU, thereby providing preclinical evidence that adjuvant anti-Notch therapy may improve outcomes for patients with malignant INS.

Materials and Methods

Cell culture

The human INS cell line CM (Baroni *et al.* 1999) was cultured in RPMI-1640 (Roswell Park Memorial Institute Media, Invitrogen, Life Technologies, Paisley, UK) supplemented with 10% foetal bovine serum (FBS) (Invitrogen) and 1% penicillin-streptomycin and plasmocin (Invitrogen). The canine INS cell line canINS was derived from a primary canine INS, TNM stage II (Buishand *et al.* 2010), resected from a 6-year old male Flatcoated Retriever at the Faculty of Veterinary Medicine, Utrecht University. Using an insulin radioimmunoassay (Cisbio, Codolet, France), it was determined that the first passage of canINS produced 305 μU/L insulin, however insulin secretion was lost after the fourth passage, like in the CM cell line. Further details on the characterisation of canINS can be found in the Supplementary data 1 (Fig. S1-2). canINS was cultured in RPMI-1640 supplemented with 10% FBS, 1% penicillin-streptomycin, 200ng/mL growth hormone (GH) (Source Biosciences, Nottingham, UK). Both lines were cultured at 37°C with 5% CO_2 and cells were passaged on reaching 70-80% confluence. Cell lines were authenticated using Short tandem repeat analysis (Cell Check Human 9 and Cell Check Canine; IDEXX Bioresearch, Windsor, UK). All experiments were conducted with cells from passage numbers 5-25.

Tumoursphere culture

Spheres were grown in serum-free medium at a density of 60,000 cells/well (2 mL volume) in 6-well low adherence plates (Corning, New York, USA). The medium consisted of DMEM/F12 (Invitrogen) supplemented with progesterone (20 nM), putrescine (100 μ M), sodium selenite (30 nM), transferrin (25 μ g/mL), insulin (20 μ g/mL) (Sigma-Aldrich, Dorset, UK). Every two days, human recombinant EGF (10 ng/mL) and human recombinant basic

fibroblast growth factor (bFGF) (10 ng/mL) (Peprotech, London, UK) were added. Spheres were passaged every week up until 15 passages. All experiments were conducted in triplicate.

RNA extraction and quantitative real time PCR

Total cellular RNA was extracted using RNeasy® kit (Qiagen, Redwood City, CA, USA) and was reverse transcribed using the Omniscript™ RT Kit (Qiagen) according to the manufacturer's instructions. Quantitative real time PCR (qRT-PCR) was performed for genes of interest by using the Stratagene M63000p qPCR system (Agilent, Santa Clara, CA, USA), and the PlatinumH SYBRH Green qPCR SuperMix-UDG (Invitrogen) according to manufacturer's instructions (primers are listed in Supplementary Tables 1 and 2). Relative gene expression levels were obtained by normalisation to the expression levels of housekeeping gene *GADPH*. Calculations were made using the Delta Delta Ct Method.

Protein extraction and western blotting

Cells were lysed in urea lysis buffer (7 M urea, 0.1 M DTT, 0.05% Triton X-100, 25 mM NaCl, 20 mM Hepes pH 7.5). Then cells were transferred to 0.1 mL Bioruptor®Microtubes (Diagenode, Seraing, Belgium) and sonicated using pre-chilled Bioruptor® Pico sonicator (Diagenode) following the manufacturer's instructions. Equal amounts of protein were separated by SDS polyacrylamide gel electrophoresis (SDS PAGE), transferred to Hybond-C nitrocellulose membrane (Amersham Pharmacia Biotech, Buckinghamshire, UK) and hybridised to the appropriate primary antibody and HRP-conjugated secondary antibody for subsequent detection by ECL. Antibodies used against HES1 (EPR4226) (1:600), Beta actin (AC-15) (1:5000), SOX9 (ab26414) (1:500) and OCT4 (ab18976) (1:1000) were purchased from Abcam (UK). Secondary antibodies were obtained from Dako (Glostrup, Denmark)

(Goat anti-Rabbit-HRP; Rabbit anti-Mouse-HRP). The appropriate secondary antibody was diluted 1:1000 (Rabbit anti-Mouse-HRP) or 1:2000 (Goat anti-Rabbit-HRP).

Choriollantoic membrane assay

Fertilised ISA Brown layer strain chicken eggs (Roslin Institute Poultry Unit, UK) were incubated in a humidified rotary incubator (Brinsea Octagon 40 OX incubator) at 37^{o}C. As chick embryo chorioallantoic membrane experimental protocols were conducted and concluded during the first two-thirds of the incubation of the embryonated eggs, according to the UK Animals (Scientific Procedures) Act 1986 regulated by the Home Office, we did not require a licence (Home Office 2014).

On day 7, single cell suspensions of trypsinised adherent CM and canINS cells or spheres were fluorescently labelled with PKH26 (Sigma-Aldrich, Dorset, UK) according to manufacturers' instructions. Cells ($1x10^4$ for each condition) were suspended in a 1:1 mixture of serum-free media and Matrigel Phenol Red Free (Corning) and 25 µL was pipette-inoculated directly onto the CAM. The shell windows were resealed and incubated without turning. At day 11, pictures were taken using Axio ZoomV16 coupled with AxioCAM HRM camera (Zeiss, Cambridge, UK). Images were processed using Zeiss pro image software and then the fluorescence was calculated using ImageJ 1.46 software (open source). All data were subtracted of background fluorescence and then averaged.

The embryos were decapitated and the area of the CAM inoculated with the fluorescent cells was harvested and stored in 10% neutral buffered formalin solution (Sigma-Aldrich) and embedded in an agarose block for cutting and staining. The staining was performed with anti-cytokeratin (MNF116; Dako) as primary antibody at 1:50 dilution for 30 min followed by staining with secondary antibody Envision anti-Mouse HRP (Dako). Images were taken using a Nikon Eclipse Ni Brightfield Microscope and thereafter processed with Zeiss pro image software (Zeiss).

Invasion assay

The invasive ability of cells was determined using the QCM™ collagen-based cell invasion assay kit (Millipore, Billerica, MA, USA) according to manufacturer's instructions. Briefly, cells were seeded into the upper inserts at 1×10^5 cells per insert in serum-free RPMI. Cells were incubated at 37 °C with 5% CO_2 for 48 hours. Non-invading cells were removed. Cells that migrated through the gel insert to the lower surface were stained and quantified by colorimetric measurement at 560 nm. Images were taken using an Eclipse Ni Brightfield Microscope (Nikon UK Ltd., Surrey, UK) and thereafter processed with Zeiss pro image software (Zeiss).

Flow cytometry

CM and canINS were detached by trypsinisation, washed with PBS and stained with the Zombie Violet Fixable Viability Kit (BioLegend Inc., San Diego, CA, USA) to detect dead cells. Subsequently, cells were washed again with PBS and fixed in paraformaldehyde at 1% for 10 min at 37°C and then chilled for one minute on ice. A batch of cells was also permeabilised by adding ice-cold 90% methanol slowly to pre-chilled cells under gentle vortexing. Cells were incubated for 30 min on ice, washed in incubation buffer (PBS 0.5% BSA) twice and resuspended in 100 μL of the diluted primary antibody at 1:800 dilution. After incubation with the primary antibody, cells were washed and incubated with a fluorochrome-conjugated secondary antibody for 30 min. After washing with incubation buffer, cells were resuspended in PBS and analysed using BD Fortessa (BD Biosciences, Oxford, UK). The primary antibody used was monoclonal anti-rabbit Notch2 (D76A6) XP® with anti-rabbit IgG (H+L) $F(ab')_2$ Fragment Alexa Fluor® 647 Conjugate (NewEnglandBio, Ipswich, MA, USA) as a secondary antibody. Rabbit (DA1E) mAb IgG XP® Isotype control Alexa Fluor® 647 Conjugate (NewEnglandBio) was used as negative control.

Growth inhibition assays

CM and canINS adherent cells and spheres were trypsinised into single cell suspensions and aliquots of 500 cells/well were seeded in triplicates in opaque 96-well plates (Corning) in 50 μL medium and incubated overnight at 37°C with 5% CO_2. After 24 hours serial dilutions of 5-FU (Tocris, R&D System, Minneapolis, Canada), or gamma-secretase inhibitor (GSI) N-[N-(3,5-Difluorophenacetyl)-L-alanyl]-S-phenylglycine t-butyl ester (DAPT) (Sigma-Aldrich) were added to the appropriate wells. Equal volumes of vehicles were used as controls. After incubation for 48 hours, cell viability was measured using the CellTiter-Glo® Luminescent Assay (Promega, Madison, WA, USA). Data of triplicate wells were averaged and normalised against the average signal of control treated samples, and dose-response curves were generated.

Colony formation assays

CM and canINS 2D and 3D cultures were trypsinised into single cell suspensions and seeded at 500 cells per 10 cm plate (Corning). Cells were treated with 5-FU and DAPT whilst in suspension. Plates were incubated at 37°C with 5% CO_2 until colonies were visible. Growth media were changed once a week. The colonies were fixed by incubating in ice-cold methanol for 5 min at room temperature. Colonies were stained with Giemsa (Invitrogen) according to the manufacturer's instructions.

Statistical analysis

All experiments were repeated at least on two separate occasions. Quantitative analysis was based on a minimum of three replicates. Data were analysed using Minitab® 17 Statistical Software (Minitab Ltd., Coventry, UK) and all graphs and diagrams were generated using Microsoft Office 2011 software (Microsoft Corporation, Redmond, WA, USA). *P*-values <0.05

239 were considered statistically significant. When data followed a normal distribution, two
240 sample *t*-tests were used to compare differences between two samples, or one-sample *t*-
241 tests to determine whether the sample mean was statistically different from a known or
242 hypothesised mean. IC_{50} values were calculated using GraphPadPrism 6 (GraphPad
243 Software, La Jolla, CA, USA). To assess combined treatment effects on the canINS and CM
244 cell lines, the Bliss additivism model was used (Buck *et al.* 2006).

245

Results

CSC-like cells are enriched in human and canine INS spheres

Human CM adherent cells (Fig. 1 A) gave rise to small and irregularly shaped spheres (Fig. 1 B), whereas canine canINS adherent cells (Fig. 1 C) gave rise to well-rounded large spheres (Fig. 1 D). These cells repeatedly formed tumourspheres for up to 15 subsequent passages when plated in low-adherent conditions. To further characterise tumourspheres we examined the expression of embryonic stem cell markers OCT4 and SOX9. Both markers were expressed at a higher level in human (Fig. 1 E) and canine (Fig. 1 F) tumourspheres compared to parental adherent cells.

We investigated the gene expression levels of a number of CSC-associated genes including stemness markers, stem cell surface related markers, epithelial-mesenchymal transition markers, growth factor receptors, Notch signalling pathway receptors and target genes, and pancreatic neuroendocrine and exocrine markers. *CD34, CD133, OCT4, SOX2, SOX9, NOTCH2, HES1* and *HEY1* were all upregulated in both human and canine INS tumourspheres compared with the adherent population (Fig. 1 G). There was no significant difference in the expression of NOTCH1, NOTCH3 and NOTCH 4 in both human and canine INS spheres, although these receptors demonstrated a trend to be downregulated in tumourspheres.

INS CSC-enriched tumourspheres are highly invasive in vitro

The invasive capacity of cells was tested *in vitro* using a collagen-based invasion assay. CSC-like cells displayed a greater invasive potential compared to the non-enriched CSCs (Fig. 2 A). When quantified, a statistically significant increased invasive potential was recorded for both human and canine INS CSC-like cells compared with non-enriched CSCs (Fig. 2 B-C).

INS CSC-enriched tumourspheres are more tumourigenic and invasive in vivo than adherent cells

We developed a CAM assay protocol to monitor the tumourigenic and metastatic properties of INS cancer cells. We recorded the amount of fluorescence in triplicate CAMs for both the adherent cells and the CSC-enriched spheres and showed that the adherent INS cells did not form tumours and did not proliferate in the CAM model. However, the CSC-like populations proliferated on the CAM and gave rise to substantial tumours (Fig. 3 A-B). We quantified the red fluorescence recorded in the CAM assay and obtained a statistical significant difference for the amount of cells between the canINS adherent and CSC-like cells (Fig. 3 C). No statistical difference was recorded between both cell populations of the human INS cell line (Fig. 3 D).

We then tested whether the cells were able to migrate through the deep layers of the CAM. Human and canine bulk INS cells (Fig. 4 A-B) were less invasive *in vivo* compared to human and canine INS CSC-like cells (Fig. 4 C-D). INS CSC-like cells demonstrated invasive behaviour moving from the outer ectoderm CAM layer through the mesoderm towards the endoderm (Fig. 4 E-F). These findings were consistent with our *in vitro* invasion data.

INS CSC-enriched tumourspheres exhibit greater resistance to 5-FU compared with adherent cells

After testing a set of chemotherapeutics commonly used in the treatment of human INS we identified 5-FU as the most suitable drug to evaluate the INS cancer cells' chemoresistance. The relative IC_{50} values for 5-FU of adherent CM and canINS cells were 5 μM and 0.5 μM, respectively, which reside within, or are lower than the therapeutic plasma dose range of 5-FU (800 ng/mL-2000 ng/mL, 5 μM-15 μM) (Danquechin-dorval et al., 1996; Yamada, 2003;

297 Blaschke et al., 2012). Both CM and canINS CSC-enriched tumourspheres proved to be
298 more resistant to 5-FU treatment compared to adherent cells in cell viability (Fig.5 A-B) and
299 clonogenicity assays (Fig. 5 C-D).
300
301 ***The Notch pathway is overexpressed and active in 5-FU resistant INS cells***
302 Analysis of gene expression had revealed that Notch pathway related receptor, NOTCH2,
303 and its target gene, HES1 were upregulated in both CM and canINS CSC-enriched spheres
304 (Fig. 1 G). Using flow cytometry, we provided evidence that the NOTCH2 receptor is
305 constitutively activated as it is present both in its inactive form (extracellular level) and active
306 form (intracellular level) in adherent and CSC-enriched sphere populations (Fig. 6 A-B).
307 Using western blot analysis, we showed that both CM and canINS CSC-enriched spheres
308 demonstrated an intrinsic higher expression of NOTCH2 and HES1 compared to the
309 adherent INS cells. Furthermore, treatment of cells with 5-FU resulted in an increased
310 expression of both the inactive and active form of the NOTCH2 receptor in CM (Fig. 6 C) and
311 canINS cells (Fig. 6 D). In response to an increase in NOTCH2 expression, also its
312 downstream target gene HES1 demonstrated an increased expression in cells that were
313 resistant to 5-FU (Fig. 6 C-D).

314

315 ***Inhibition of Notch signalling decreases viability and 5-FU resistance in INS CSC-***
316 ***enriched tumourspheres***

317 Since CSC-enriched INS spheres were more resistant to 5-FU treatment compared to
318 adherent cells and 5-FU resistant INS cells demonstrated an overexpression of active
319 NOTCH2, we evaluated the effect of Notch pathway inhibition on INS cells. Notch
320 inhibition using DAPT, preferentially decreased the viability of CM and canINS CSC-
321 enriched spheres (Fig. 7 A-B). CSC-enriched canINS spheres demonstrated increased

sensitivity to treatment with DAPT compared with CSC-enriched CM spheres. To confirm whether the DAPT is able to specifically inhibit the Notch pathway, we treated the human and canine cells with increasing doses of DAPT and observed, through western blot analysis, a reduced expression of the intracellular form of NOTCH2 (NOTCH2-IC) and its downstream target HES1 in both human and canine INS cell lines (Fig. 7 C-D). We demonstrated that a blockade of the Notch signalling occurs in CSC-enriched canINS spheres at a lower dose of DAPT compared to CSC-enriched CM spheres (Fig. 7 C-D). Finally, when DAPT was used in combination with 5-FU, we demonstrated that the clonogenicity of CSC-enriched CM and canINS spheres was significantly reduced. This effect was superior to use of either drug alone (Fig. 7 E-F). The synergistic effect of the combination of 5-FU and DAPT was confirmed using the Bliss independence model (Fig. 7 G-H).

Notch inhibition enhances chemosensitivity to 5-FU treatment of INS CSC-enriched tumourspheres in vivo

In order to validate the results obtained *in vitro*, we tested this approach in the *in vivo* CAM model. Treatment with either 5-FU, DAPT, or their combination, in the CAM model demonstrated that the human and canine INS CSC populations were not able to proliferate when treated with a combination of 5-FU and DAPT (Fig. 8 A-B). We recorded the amount of fluorescence in the triplicate CAMs for the different conditions and demonstrated that the combination of 5-FU and DAPT significantly decreased the proliferation of INS CSC-like cells, while neither treatment with DAPT, or 5-FU alone led to a significant reduction in cell proliferation (Fig. 8 C-D).

Discussion

In the current study, we demonstrated that human and canine INS cell lines could be enriched in CSCs by tumoursphere culturing. CSCs have been previously isolated from a variety of human (Zhu *et al.* 2011; Mao *et al.* 2014; Paschall *et al.* 2016; Zhao *et al.* 2016; Sakai *et al.* 2017) and canine cancer types (Wilson *et al.* 2008; Stoica *et al.* 2009; Pang *et al.* 2011, 2012, 2017; Rybicka & Król 2016). However, to our knowledge, we are the first to report the isolation of CSC-like cells from a canine INS cell line and the use of this cell line as comparative model for human INS.

CSC-enriched tumourspheres from both species demonstrated a common upregulation of stem cell-associated markers *CD133, CD34, OCT4, SOX9,* and *SOX2.* Previously, *OCT4*, *SOX2*, *SOX9* and *CD133* have been identified as stem cell markers of pancreatic endocrine progenitor cells (Seymour *et al.* 2007; Koblas *et al.* 2008; Wang *et al.* 2009; Venkatesan *et al.* 2011). Of these markers, *CD133* expression was demonstrated to be a negative prognosticator in PancNETs (Sakai *et al.* 2017).

Human and canine CSC-like INS cells were highly invasive *in vitro*, similar to CSCs isolated in previous studies (Gaur *et al.* 2011; Pang *et al.* 2011; Gao *et al.* 2014). CSC-like INS cells displayed a greater invasive potential compared to the bulk INS cells in both *in vitro* invasion assays and *in vivo* CAM models. Previously, the CAM model has been used to model metastatic behaviour in other cancer types such as breast, bladder, prostate, ovarian cancer and head and neck cancers in humans (Deryugina *et al.* 2009; Lokman *et al.* 2012) and mammary carcinoma and osteosarcoma in companion animals (Pang *et al.* 2013, 2014). In our CAM assays, CSCs from INS tumourspheres developed visible tumours within 4 days, and escaped the primary inoculation site and migrated to the inner layers of the CAM. The invasive behaviour of INS CSCs in the CAM model with its highly vascularised structure, closely mimics the mode of INS metastasis which involves INS cancer cell invasion and

spread through the abdominal lymphatic system to reach the site of metastases in either lymph nodes or liver. Overall, these findings suggest CSCs may play a role in INS carcinogenesis.

According to our results, INS CSC-like cells are more resistant to 5-FU compared to the adherent cancer cells. This is consistent with the CSC model stating that despite the sensitivity of bulk tumour cells to chemotherapy, CSCs are resistant and lead ultimately to the failure of cytotoxic chemotherapy, increasing the need for new CSC-targeted therapies (Guo *et al.* 2006). After isolating INS CSCs, we have identified the Notch pathway as a potential target for INS CSC targeted therapy. Notch signalling pathway activation occurs when a Notch receptor (NOTCH 1–4) binds to one of the five known Notch ligands (Delta-like-1, -3, and -4 and Jagged-1 and -2). After receptor–ligand binding, there is a two-step proteolytic cleavage, first by ADAM10, then by gamma-secretase of the intracellular domain of the Notch receptor (NICD). NCID translocates to the nucleus, interacts with CSL transcription factors (CBF1/RBP-J, Su(H), Lag-1) which activate and promote transcription of downstream genes such as HES1, involved in various differentiation programmes (Grande *et al.* 2011; Abel *et al.* 2014). For instance, Notch signalling has a major role in pancreatic embryogenesis, influencing the balance between pancreatic endocrine progenitors, exocrine cells and differentiated beta-cells (Angelis *et al*. 1999; Andersson *et al*. 2011). The current study demonstrates that NOTCH2 is constitutively active in CM and canINS cells. Furthermore, *NOTCH2* and *HES1* are overexpressed in human and canine CSC-like cells, compared to the bulk INS cells. *NOTCH2* is the only Notch receptor that have demonstrated overexpression in both human and canine INS suggesting that *NOTCH2* is the most relevant Notch receptor through which signalling in INS CSCs is mediated. The role of the Notch pathway has been previously described in various types of NETs (Grande *et al.* 2011; Carter *et al.* 2013; Crabtree *et al.* 2016) but to our knowledge this is the first study to evaluate the role of the Notch pathway in INS tumourigenicity and

399 in particular its role in maintaining the INS CSC population. Previous studies have
400 identified NOTCH2 as an oncogene in NETs (Carter *et al.* 2013; Crabtree *et al.* 2016): in
401 small cell lung carcinoma (SCLC) Notch2 signalling has shown a prominent role in tumour
402 promotion in SCLC xenografts in mice (Crabtree *et al.* 2016). Recently NOTCH2
403 overexpression has been related to increased tumourigenicity of cancer cells, and an
404 increased resistance to 5-FU in hepatocellular carcinoma (Rui *et al.* 2016). In our study,
405 we have demonstrated an increased activation of the Notch pathway in INS cells, after
406 treatment with 5-FU. The observed enhancement in Notch signalling may be explained by
407 a selective enrichment of the INS 5-FU resistant cells that display an active Notch
408 signalling. In accordance with this hypothesis, previous studies have demonstrated that
409 overexpression of HES1 has been related to an increased resistance to 5-FU in colon
410 cancer (Candy *et al.* 2013) and oesophageal squamous cell carcinoma (Liu *et al.* 2013).

411 Notch signalling in CM and canINS may contribute to carcinogenesis by inhibiting
412 differentiation, promoting cellular proliferation, and/or inhibiting apoptosis, yet no studies
413 have examined these endpoints in INS. Our results showed that NOTCH2 is constitutively
414 activated in both CSC-like cells and bulk INS cells, although the bulk cancer cell
415 population demonstrated a lower expression of HES1. Interestingly, Notch inhibition using
416 DAPT preferentially decreased the viability of the CSC-like population. Considering that
417 NOTCH2 was the only overexpressed Notch receptor in human and canine INS CSCs,
418 these data suggest that the Notch2-Hes1 signalling cascade plays an important role in
419 CSCs' survival and resistance to chemotherapy. Next, we have tested whether a
420 combined regimen of DAPT and 5-FU can reverse the 5-FU resistance of INS CSC-like
421 cells. Treatment *in vitro* with DAPT alone did not inhibit INS CSC-like cells clonogenicity,
422 however, the combination of DAPT and 5-FU significantly inhibited colony-forming ability of
423 INS CSC-like cells to a greater degree than either therapy alone. We have then used the

CAM model to study the effect of this combined treatment *in vivo*. The results from the CAM assay were consistent with the *in vitro* findings, as tumour proliferation *in vivo* was significantly decreased when the drugs were used in combination compared to their use as single agents. Previous studies have already shown that Notch inhibition increased the cytotoxic effects of chemotherapy in various types of cancer (Meng *et al*. 2009; Lee *et al*. 2015; Li *et al*. 2015): for example oxaliplatin-induced activation of Notch1 signalling in metastatic colon cancer was reduced by simultaneous GSI treatment, resulting in enhanced tumour sensitivity to oxaliplatin (Meng *et al.* 2009); in breast cancer, combined inhibition of Notch with doxorubicin treatment resulted in decreased tumourigenicity in mouse xenograft models (Li *et al.* 2015); and in gastric cancer, targeting the Notch pathway significantly increased the cytotoxicity of 5-FU (Lee *et al.* 2015). Demonstrating that inhibition of the Notch pathway has functional consequences provides further evidence that this pathway is not only differentially expressed but plays a causative role in INS carcinogenesis.

In summary, in the current study, we have isolated INS CSC-like cells from human and canine INS cell lines and have demonstrated that both subpopulations of INS CSC-like cells seem to be dependent on the Notch pathway for their survival. Furthermore, targeting the Notch pathway led to a significant increase in cytotoxicity of 5-FU in the INS CSC-like population, demonstrating a correlation between Notch activation and 5-FU resistance. The increased expression of Notch in 5-FU resistant INS cells may be clinically significant, as it provides a valuable rationale that INS patients whom developed chemoresistance might benefit from a treatment with Notch small molecule inhibitors, such as GSIs. GSI treatment has previously been used in a clinical setting to sensitise cancer cells to chemotherapy in advanced stages of solid tumours (Richter *et al.* 2014). Since GSIs including DAPT, inhibit cleavage of all Notch receptor families, our results may not be

exclusively due to Notch2 signalling effects. Therefore, future preclinical studies on INS will focus on the use of specific inhibitors of either NOTCH2 or HES1, and further, elucidate their potential in clinical settings.

Declaration of interest

The authors declare that there is no conflict of interest that could be perceived as prejudicing the impartiality of the research reported.

Funding

This work was supported by the Morris Animal Foundation (grant number: D14CA-503).

Authors contributions

J.K., J.A.M., F.O.B., L.Y.P. and D.J.A conceived the study; Y.C., F.O.B., L.Y.P., J.A.M. and D.J.A designed the experiments. Y.C. performed the experiments and analysed the data, interpreted the results and drafted the manuscript. Y.C. and F.O.B. wrote the final version of the manuscript. L.Y.P., J.K., J.A.M. and D.J.A. revised and reviewed the manuscript.

Acknowledgements

Authors would like to thank Dr. Anna Raper, Dr. Breno Beirao, Dr. Karen Tan, Dr. Mark Woodcock, Dr. Richard Elders, Dr. Steven Meek and Mr. Robert Fleming for the technical support and advice throughout the experimental design. Authors would also like to thank Mr. Neil MacIntyre and the R(D)SVS pathology laboratory for cutting and staining the CAM and Mrs. Rhona Muirhead for the technical support.

References

Abel E V., Kim EJ, Wu J, Hynes M, Bednar F, Proctor E, Wang L, Dziubinski ML & Simeone DM 2014 The notch pathway is important in maintaining the cancer stem cell population in pancreatic cancer. *PLoS ONE* **9** 1–13. (doi:10.1371/journal.pone.0091983)

Andersson ER, Sandberg R & Lendahl U 2011 Notch signaling: simplicity in design, versatility in function. *Development (Cambridge, England)* **138** 3593–3612. (doi:10.1242/dev.063610)

Angelis D, Lendahl U, Hrabe M & Edlund H 1999 Notch signalling controls pancreatic cell differentiation. **400** 14–16.

Athanasopoulos PG, Polymeneas G, Dellaportas D, Mastorakos G, Kairi E & Voros D 2011 Concurrent insulinoma and pancreatic adenocarcinoma: report of a rare case and review of the literature. *World Journal of Surgical Oncology* **9** 7. (doi:10.1186/1477-7819-9-7)

Bailey DB & Page RL 2007 *Withrow & MacEwen's Small Animal Clinical Oncology*. Elsevier Inc. (doi:10.1016/B978-072160558-6.50027-7)

Baroni MG, Cavallo MG, Mark M, Monetini L, Stoehrer B & Pozzilli P 1999 Beta-cell gene expression and functional characterisation of the human insulinoma cell line CM. 59–68.

Baudin E, Caron P, Lombard-Bohas C, Tabarin A, Mitry E, Reznick Y, Taieb D, Pattou F, Goudet P, Vezzosi D *et al.* 2014 [Malignant insulinoma: recommendations for workup and treatment]. *Presse Médicale (Paris, France : 1983)* **43** 645–659. (doi:10.1016/j.lpm.2013.08.007)

Blaschke M, Blumberg J, Wegner U, Nischwitz M, Ramadori G & Cameron S 2012 Measurements of 5-FU Plasma Concentrations in Patients with Gastrointestinal Cancer: 5-FU Levels Reflect the 5-FU Dose Applied. *Journal of Cancer Therapy* **3** 28–36. (doi:10.4236/jct.2012.31004)

Bomken S, Fiser K, Heidenreich O, Vormoor J 2010 Understanding the cancer stem cell. *Br J Cancer* **103** 439-445.

Buck E, Eyzaguirre A, Brown E, Petti F, McCormack S, Haley JD, Iwata KK, Gibson NW & Griffin G. 2006. Rapamycin synergizes with the epidermal growth factor receptor inhibitor erlotinib in non-small-cell lung, pancreatic, colon, and breast tumors. *Mol Cancer Ther* **5** 2676-2684.

499 Buishand FO, Kik M & Kirpensteijn J 2010 Evaluation of clinico-pathological criteria and the Ki67
500 index as prognostic indicators in canine insulinoma. *The Veterinary Journal* **185** 62–67.
501 (doi:10.1016/j.tvjl.2010.04.015)

502 Buishand FO, Kirpensteijn J, Jaarsma A a, Speel E-JM, Kik M & Mol J a 2013 Gene expression
503 profiling of primary canine insulinomas and their metastases. *Veterinary Journal (London,*
504 *England : 1997)* **197** 192–197. (doi:10.1016/j.tvjl.2013.01.021)

505 Buishand FO, Visser J, Kik M, Gröne A, Keesler RI, Briaire-de Bruijn IH & Kirpensteijn J 2014
506 Evaluation of prognostic indicators using validated canine insulinoma tissue microarrays.
507 *Veterinary Journal (London, England : 1997)* **201** 57–63. (doi:10.1016/j.tvjl.2014.05.004)

508 Callacondo D, Arenas JL, Ganoza AJ, Rojas-Camayo J, Quesada-Olarte J & Robledo H 2013
509 Giant insulinoma: a report of 3 cases and review of the literature. *Pancreas* **42** 1323–1332.
510 (doi:10.1097/MPA.0b013e318292006a)

511 Candy P a, Phillips MR, Redfern a D, Colley SM, Davidson J a, Stuart LM, Wood B a, Zeps N &
512 Leedman PJ 2013 Notch-induced transcription factors are predictive of survival and 5-
513 fluorouracil response in colorectal cancer patients. *British Journal of Cancer* **109** 1023–1030.
514 (doi:10.1038/bjc.2013.431)

515 Carter Y, Jaskula-sztul R, Chen H & Mazeh H 2013 Signaling pathways as specific pharmacologic
516 targets for neuroendocrine tumor therapy: RET, PI3K, MEK, growth factors, and Notch.
517 *Neuroendocrinology* **97** 57–66. (doi:10.1159/000335136.Signaling)

518 Corroller AB, Valéro R, Moutardier V, Henry J, Treut Y Le, Gueydan M, Micco C De, Sierra M,
519 Conte-devolx B, Oliver C *et al.* 2008 Aggressive multimodal therapy of sporadic malignant
520 insulinoma can improve survival : A retrospective 35-year study of 12 patients. *Diabetes &*
521 *Metabolism* **34** 343–348. (doi:10.1016/j.diabet.2008.01.013)

522 Crabtree JS, Singleton CS & Miele L 2016 Notch Signaling in Neuroendocrine Tumors. *Frontiers in*
523 *Oncology* **6** 94. (doi:10.3389/fonc.2016.00094)

524 Danquechin-dorval EM & Gesta PH 1996 Intensity and Therapeutic Response in Patients with
525 Advanced Colorectal Cancer Receiving Infusional Therapy Containing 5-FU. *Cancer* **77** 441–

451.

Deryugina EI & Quigley JP 2009 Chick embryo chorioallantoic membrane model systems to study and visualize human tumor cell metastasis. *Cell* **130** 1119–1130. (doi:10.1007/s00418-008-0536-2.Chick)

Gao F, Zhang Y, Wang S, Liu Y, Zheng L, Yang J, Huang W, Ye Y, Luo W & Xiao D 2014 Hes1 is involved in the self-renewal and tumourigenicity of stem-like cancer cells in colon cancer. *Scientific Reports* **4** 3963. (doi:10.1038/srep03963)

Gaur P, Sceusi EL, Samuel S, Xia L, Fan F, Zhou Y, Lu J, Tozzi F, Lopez-Berestein G, Vivas-Mejia P *et al.* 2011 Identification of cancer stem cells in human gastrointestinal carcinoid and neuroendocrine tumors. *Gastroenterology* **141** 1728–1737. (doi:10.1053/j.gastro.2011.07.037)

Gordon I, Paoloni M, Mazcko C & Khanna C 2009 The comparative oncology trials consortium: Using spontaneously occurring cancers in dogs to inform the cancer drug development pathway. *PLoS Medicine* **6** 2–6. (doi:10.1371/journal.pmed.1000161)

Goutal CM, Brugmann BL & Ryan K a 2012 Insulinoma in dogs: a review. *Journal of the American Animal Hospital Association* **48** 151–163. (doi:10.5326/JAAHA-MS-5745)

Grande E, Capdevila J, Barriuso J, Antón-Aparicio L & Castellano D 2011 Gastroenteropancreatic neuroendocrine tumor cancer stem cells: do they exist? *Cancer and Metastasis Reviews* **31** 47–53. (doi:10.1007/s10555-011-9328-6)

Guo W, Lasky JL & Wu H 2006 Cancer stem cells. *Pediatric Research* **59** 59R–64R. (doi:10.1203/01.pdr.0000203592.04530.06)

Home Office 2014 *Guidance on the Operation of the Animals (Scientific Procedures) Act 1986*. (doi:ISBN 1474100287- 9781474100281)

Hou Y-C, Chao Y-J, Tung H-L, Wang H-C & Shan Y-S 2014 Coexpression of CD44-positive/CD133-positive cancer stem cells and CD204-positive tumor-associated macrophages is a predictor of survival in pancreatic ductal adenocarcinoma. *Cancer* **120** 2766–2777. (doi:10.1002/cncr.28774)

552 Jonkers YMH, Ramaekers FCS & Speel EJM 2007 Molecular alterations during insulinoma
553 tumorigenesis. *Biochimica et Biophysica Acta* **1775** 313–332.
554 (doi:10.1016/j.bbcan.2007.05.004)

555 Katz R, Manikam R SL 2006 *Pediatric and Adolescent*.

556 Koblas T, Pektorova L, Zacharovova K, Berkova Z, Girman P, Dovolilova E, Karasova L & Saudek
557 F 2008 Differentiation of CD133-Positive Pancreatic Cells Into Insulin-Producing Islet-Like
558 Cell Clusters. *Transplantation Proceedings* **40** 415–418.
559 (doi:10.1016/j.transproceed.2008.02.017)

560 Krampitz GW, George BM, Willingham SB, Volkmer J-P, Weiskopf K, Jahchan N, Newman AM,
561 Sahoo D, Zemek AJ, Yanovsky RL *et al.* 2016 Identification of tumorigenic cells and
562 therapeutic targets in pancreatic neuroendocrine tumors. *Proceedings of the National*
563 *Academy of Sciences of the United States of America* **113** 4464–4469.
564 (doi:10.1073/pnas.1600007113)

565 Li Z-L, Chen C, Yang Y, Wang C, Yang T, Yang X & Liu S-C 2015 Gamma secretase inhibitor
566 enhances sensitivity to doxorubicin in MDA-MB-231 cells. *International Journal of Clinical and*
567 *Experimental Pathology* **8** 4378–4387.

568 Liu J, Fan H, Ma Y, Liang D, Huang R, Wang J, Zhou F, Kan Q, Ming L, Li H *et al.* 2013 Notch1 Is
569 a 5-Fluorouracil Resistant and Poor Survival Marker in Human Esophagus Squamous Cell
570 Carcinomas. *PLoS ONE* **8**. (doi:10.1371/journal.pone.0056141)

571 Lokman NA, Elder ASF, Ricciardelli C & Oehler MK 2012 Chick chorioallantoic membrane (CAM)
572 assay as an in vivo model to study the effect of newly identified molecules on ovarian cancer
573 invasion and metastasis. *International Journal of Molecular Sciences* **13** 9959–9970.
574 (doi:10.3390/ijms13089959)

575 Mao Z, Liu J, Mao Z, Huang J, Xie S & Liu T 2014 Blocking the NOTCH pathway can inhibit the
576 growth of CD133-positive A549 cells and sensitize to chemotherapy. *Biochemical and*
577 *Biophysical Research Communications* **444** 670–675. (doi:10.1016/j.bbrc.2014.01.164)

578 Mathur A, Gorden P & Libutti S 2012 Insulinoma. **89** 1105–1121.

(doi:10.1016/j.suc.2009.06.009.Insulinoma)

Meng RD, Shelton CC, Li YM, Qin LX, Notterman D, Paty PB & Schwartz GK 2009 ??-secretase inhibitors abrogate oxaliplatin-induced activation of the Notch-1 signaling pathway in colon cancer cells resulting in enhanced chemosensitivity. *Cancer Research* **69** 573–582. (doi:10.1158/0008-5472.CAN-08-2088)

Mitra A, Mishra L & Li S 2015 EMT , CTCs and CSCs in tumor relapse and drug-resistance. *Oncotarget* **6** 10697–10711.

Ordóñez NG, 2001 Insulinoma with fibrillar inclusions and acinar cell elements. *Ultrastructural Pathology* **25** 485–495.

Pang LY, Cervantes-Arias A, Else RW & Argyle DJ 2011 Canine Mammary Cancer Stem Cells are Radio- and Chemo- Resistant and Exhibit an Epithelial-Mesenchymal Transition Phenotype. *Cancers* **3** 1744–1762. (doi:10.3390/cancers3021744)

Pang LY, Bergkvist GT, Cervantes-Arias a, Yool D a, Muirhead R & Argyle DJ 2012 Identification of tumour initiating cells in feline head and neck squamous cell carcinoma and evidence for gefitinib induced epithelial to mesenchymal transition. *Veterinary Journal (London, England : 1997)* **193** 46–52. (doi:10.1016/j.tvjl.2012.01.009)

Pang LY, Blacking TM, Else RW, Sherman A, Sang HM, Whitelaw BA, Hupp TR & Argyle DJ 2013 Feline mammary carcinoma stem cells are tumorigenic, radioresistant, chemoresistant and defective in activation of the ATM/p53 DNA damage pathway. *Veterinary Journal* **196** 414–423. (doi:10.1016/j.tvjl.2012.10.021)

Pang LY, Gatenby EL, Kamida A, Whitelaw B a, Hupp TR & Argyle DJ 2014 Global gene expression analysis of canine osteosarcoma stem cells reveals a novel role for COX-2 in tumour initiation. *PloS One* **9** e83144. (doi:10.1371/journal.pone.0083144)

Pang LY, Saunders L & Argyle DJ 2017 Edinburgh Research Explorer Epidermal Growth Factor Receptor activity is elevated in glioma cancer stem cells and is required to maintain chemotherapy and radiation resistance. *Oncotarget*.

605 Paschall A V, Yang D, Lu C, Redd PS, Choi J & Christopher M 2016 CD133 + CD24 lo defines a
606 5-Fluorouracil-resistant colon cancer stem cell-like phenotype. **7**.
607 (doi:10.18632/oncotarget.12168)

608 Polton G a, White RN, Brearley MJ & Eastwood JM 2007 Improved survival in a retrospective
609 cohort of 28 dogs with insulinoma. *The Journal of Small Animal Practice* **48** 151–156.
610 (doi:10.1111/j.1748-5827.2006.00187.x)

611 Richter S, Bedard PL, Chen EX, Clarke B a., Tran B, Hotte SJ, Stathis A, Hirte HW, Razak AR a,
612 Reedijk M *et al.* 2014 A phase i study of the oral gamma secretase inhibitor R04929097 in
613 combination with gemcitabine in patients with advanced solid tumors (PHL-078/CTEP 8575).
614 *Investigational New Drugs* **32** 243–249. (doi:10.1007/s10637-013-9965-4)

615 Rui W, Xiang de S, bo LX, Liu C & Zhang R 2016 Notch2 Regulates Self-Renewal and
616 Tumorigenicity of Human Hepatocellular Carcinoma Cells. *Journal of Hepatology* **64** S577–
617 S578. (doi:10.1016/S0168-8278(16)01055-2)

618 Rybicka A & Król M 2016 Identification and characterization of cancer stem cells in canine
619 mammary tumors. *Acta Veterinaria Scandinavica* **58** 86. (doi:10.1186/s13028-016-0268-6)

620 Sakai Y, Hong S-M, An S, Kim JY, Corbeil D, Karbanová J, Otani K, Fujikura K, Song K-B, Kim SC
621 *et al.* 2017 CD133 expression in well-differentiated pancreatic neuroendocrine tumors: a
622 potential predictor of progressive clinical courses. *Human Pathology* **61** 148–157.
623 (doi:10.1016/j.humpath.2016.10.022)

624 Schiffman JD & Breen M 2015 Comparative oncology: what dogs and other species can teach us
625 about humans with cancer. *Philosophical Transactions of the Royal Society B: Biological*
626 *Sciences* **370** 20140231–20140231. (doi:10.1098/rstb.2014.0231)

627 Seymour P a, Freude KK, Tran MN, Mayes EE, Jensen J, Kist R, Scherer G & Sander M 2007
628 SOX9 is required for maintenance of the pancreatic progenitor cell pool. *Proceedings of the*
629 *National Academy of Sciences of the United States of America* **104** 1865–1870.
630 (doi:10.1073/pnas.0609217104)

631 Speel EJM, Richter J, Moch H, Egenter C, Saremaslani P, Rütimann K, Zhao J, Barg-Horn A, Roth

J, Heitz PU, Komminoth P 1999 Genetic differences in endocrine pancreatic tumor subtypes detected by comparative genomic hybridization. *American Journal of Pathology* **155** 1787-1794.

Stoica G, Lungu G, Martini-Stoica H, Waghela S, Levine J & Smith R 2009 Identification of cancer stem cells in dog glioblastoma. *Veterinary Pathology* **46** 391–406. (doi:10.1354/vp.08-VP-0218-S-FL)

Venkatesan V, Gopurappilly R, Goteti SK, Dorisetty RK & Bhonde RR 2011 Pancreatic progenitors: The shortest route to restore islet cell mass. *Islets* **3** 295–301. (doi:10.4161/isl.3.6.17704)

Wang XC, Xu SY, Wu XY, Song HD, Mao YF, Fan HY, Yu F, Mou B, Gu YY, Xu LQ *et al.* 2004 Gene expression profiling in human insulinoma tissue: Genes involved in the insulin secretion pathway and cloning of novel full-length cDNAs. *Endocrine-Related Cancer* **11** 295–303. (doi:10.1677/erc.0.0110295)

Wang H, Wang S, Hu J, Kong Y, Chen S, Li L & Li L 2009 Oct4 is expressed in Nestin-positive cells as a marker for pancreatic endocrine progenitor. *Histochemistry and Cell Biology* **131** 553–563. (doi:10.1007/s00418-009-0560-x)

Wilson H, Huelsmeyer M, Chun R, Young KM, Friedrichs K & Argyle DJ 2008 Isolation and characterisation of cancer stem cells from canine osteosarcoma. *Veterinary Journal (London, England : 1997)* **175** 69–75. (doi:10.1016/j.tvjl.2007.07.025)

Yamada Y 2003 Plasma concentrations of 5-fluorouracil and F- b -alanine following oral administration of S-1 , a dihydropyrimidine dehydrogenase inhibitory fluoropyrimidine , as compared with protracted venous infusion of 5-fluorouracil. *British Journal of Cancer* **89** 816–820. (doi:10.1038/sj.bjc.6601224)

Zhao J, Moch AF, Scheidweiler AF, Baer AA, Schaffer AA, Speel EJ, Roth J, Heitz PU, Komminoth P 2001 Genomic imbalances in the progression of endocrine pancreatic tumors. *Genes Chromosomes Cancer* **32** 364-372.

Zhao Z-L, Zhang L, Huang C-F, Ma S-R, Bu L-L, Liu J-F, Yu G-T, Liu B, Gutkind JS, Kulkarni AB *et*

659 *al.* 2016 NOTCH1 inhibition enhances the efficacy of conventional chemotherapeutic agents
660 by targeting head neck cancer stem cell. *Scientific Reports* **6** 24704. (doi:10.1038/srep24704)

661 Zhu TS, Costello M a., Talsma CE, Flack CG, Crowley JG, Hamm LL, He X, Hervey-Jumper SL,
662 Heth J a., Muraszko KM *et al.* 2011 Endothelial cells create a stem cell niche in glioblastoma
663 by providing NOTCH ligands that nurture self-renewal of cancer stem-like cells. *Cancer*
664 *Research* **71** 6061–6072. (doi:10.1158/0008-5472.CAN-10-4269)

665

666

Figure legends

Figure 1 Isolation and characterisation of CM and canINS cancer stem cells (CSC). **A-B**: CM in adherent (A) and in tumoursphere (B) culturing conditions (scale bar: 100 □m). **C-D**: canINS in adherent (C) and tumoursphere (D) culturing conditions (scale bar: 100 □m). **E-F**: Western blot analysis of CM (E) and canINS (F) stem cell markers OCT4 and SOX9 and beta actin as loading control. **G:** qRT-PCR of stem cell and self-renewal pathway related genes comparing CM and canINS in both adherent and sphere culturing conditions. The mRNA expression of embryonic stem cell genes (SOX9, OCT4, SOX2) and stem cell-associated surface markers (CD133, CD34) were upregulated in sphere culturing conditions. The expression of NOTCH receptor (NOTCH2) and downstream target genes (HES1, HEY1) was upregulated, whereas no significant differences were recorded in NOTCH1, NOTCH3 and NOTCH4 expression in human and canine INS spheres. Values are mean of triplicates ± SD. The P-values represent the comparison with a stated hypothesis (values >1) using one samples t-test. *P-values <0.05 were considered statistically significant.

Figure 2 Invasive properties of INS CSCs in vitro**. A:** Representative images of invasive capacity of human (top row) and canine (bottom row) CSC-enriched spheres and adherent cells using a collagen-based cell invasion assay kit (scale bar: 20 □m) **B-C**: Invading cells were stained and quantified by colourimetric measurement at 560 nm. Values are mean of 3 ± SEM. *P-value < 0.05.

Figure 3 Putative canine and human INS CSCs show an increased in vivo tumourigenic potential **A**: Representative photographs of the chorioallantoic membrane (CAM) 11 days after inoculation with either canINS adherent cells or CSC-enriched spheres following red fluorescent membrane labelling. Pictures on the top row show the merging of the brightfield channel; pictures on the bottom row show the red channel. A3 represents a magnified picture

of the circles shown in A2. Magnification is specified on top of each picture. **B**: Representative photographs of the chorioallantoic membrane (CAM) 11 days after inoculation with either CM adherent cells or CSC-enriched spheres following red membrane labelling. C3 represents magnified pictures of the circles shown in C2. **C-D:** Graphs show the differences in fluorescence between the two populations after quantification using ImageJ. Values are mean of 3 ± SEM. *P-value < 0.05.

Figure 4 Invasive properties of INS CSCs in vivo. **A-F:** Representative images of immunohistochemistry of CAM sections embedded in agar and stained with anti-cytokeratin that stains only human and canine cells (brown). The structure of CAM layers is comprised by ectoderm (ET), mesoderm (M) and endoderm (ED). Cancer cell matrigel grafts (CG) were seeded on the CAM. Pictures show the migration of CM adherent (A) and canINS adherent (B) and CM CSC-enriched sphere cells (C) and canINS CSC-enriched sphere cells (D) in the inner part of the CAM 11 days after being seeded. Results show that the CM adherent (A) and the canINS adherent (B) migrate less through the different layers of the CAM compared with the CM CSC-enriched sphere cells (C) and the canINS CSC-enriched sphere cells (D). High magnifications (20x and 60x) shows in details how the CM (E) and canINS (F) CSC-enriched sphere cells disrupt the CAM membrane and invade through the CAM layers. Magnification is specified on top of each picture (scale bar: 200 □m).

Figure 5 Chemosensitivity and colony formation assays of CM and canINS. **A-B**: Chemosensitivity assay in CM (A) and canINS (B): cells were treated with increasing concentrations of 5-FU (from 0.5 to 5 μM) comparing the adherent population (dashed line) and the CSC-enriched sphere population (continuous line). **C-D**: Colony formation assay CM (C) and canINS (D): Human and canine cells were treated with increasing concentrations of

5-FU (from 0.5 to 5 μM) comparing the adherent population (dashed) and the CSC-enriched sphere population (solid). Values represent mean of triplicates ± SD. The P-values represent the comparison using 2 sample t-test within the adherent and the CSC-enriched spheres. *P-value < 0.05 was considered statistically significant.

Figure 6 Analysis of Notch pathway protein expression and activation in human and canine insulinoma (INS) cells. **A-B**: Graph showing the percentage of cells positive to NOTCH2 antibody using flow cytometry in human (A) and canine (B) INS cell lines. **C-D**: Western blot analysis of NOTCH2 in its inactive transmembrane form (NOTCH2-TM) and its active intracellular form (NOTCH2-IC), and HES1 with beta actin as a loading control in human (C) and canine (D) INS cell lines, treated with increasing doses of 5-Fluorouracil (5-FU).

Figure 7 Function of the Notch pathway in canine and human insulinoma (INS) cancer stem cells (CSC). **A-B**: Cell viability assay of human (A) and canine (B) INS cell lines using increasing concentrations of DAPT comparing adherent cells (dashed line) against CSC-enriched spheres (solid line). **C-D:** Western blot analysis of NOTCH2 in its inactive transmembrane form (NOTCH2-TM) and in its active intracellular form (NOTCH2-IC), and HES1, with beta actin as a loading control in human (C) and canine (D) INS cell lines treated with increasing doses of DAPT. **E-F**: Colony formation assay of human (E) and canine (F) INS cell lines using a combination of DAPT and 5-fluorouracil (5-FU). Values represent mean of triplicates ± SD. The P-values represent the comparison using 2 sample t-tests within the adherent and the CSC-enriched spheres. *P-value < 0.05. **G-H**: Calculation of the synergistic effect of the DAPT and 5-FU using e-bliss calculation in CM (G) and canINS (H). The method compares the observed combined response with the predicted combined response. The combined effect is synergistic as it is greater than the predicted one.

Figure 8 Combined 5-FU and DAPT treatment decreases human and canine INS CSC-like cells tumourigenic potential in the in vivo chorioallantoic membrane (CAM) model**. A:** Representative photographs of the CAM 11 days after inoculation with CSC-enriched CM spheres following red membrane labelling. Cells have been treated with 5-FU (5 µM) and DAPT (20 µg/mL). Pictures on the top row show the merging of the brightfield channel; pictures on the bottom row show the red channel (scale bar: 100µm). **B**: Representative photographs of the CAM 11 days after inoculation with CSC-enriched canINS spheres following red membrane labelling. Cells have been treated with 5-FU (0.5 µM) and DAPT (20 µg/ml). Pictures on the top row show the merging of the brightfield channel; pictures on the bottom row show the red channel (scale bar: 100µm). **C-D:** Graphs show the differences in fluorescence between the different conditions after quantification using ImageJ. Values are the mean of 3 ± SEM. *P-value < 0.05.

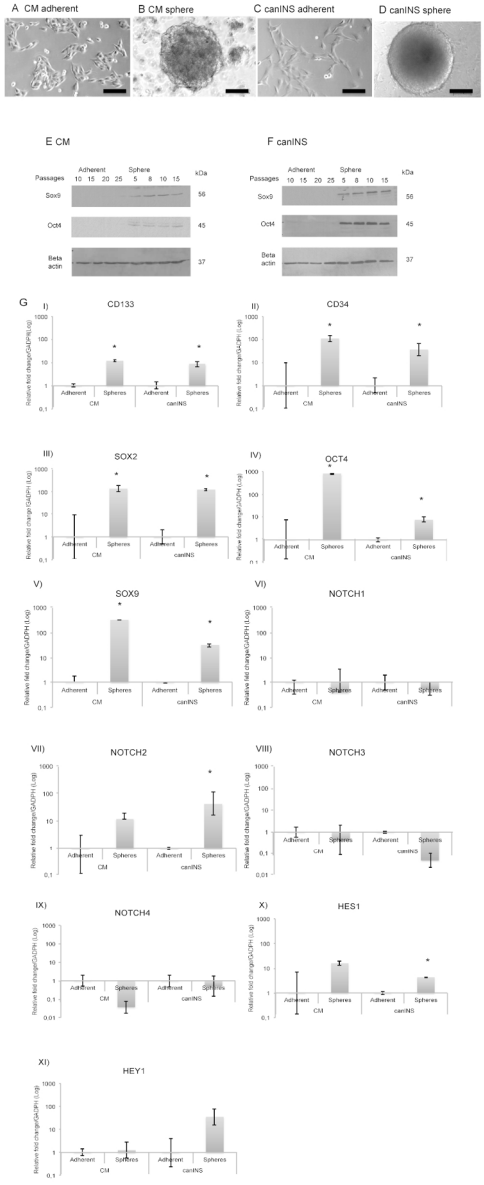

192x423mm (150 x 150 DPI)

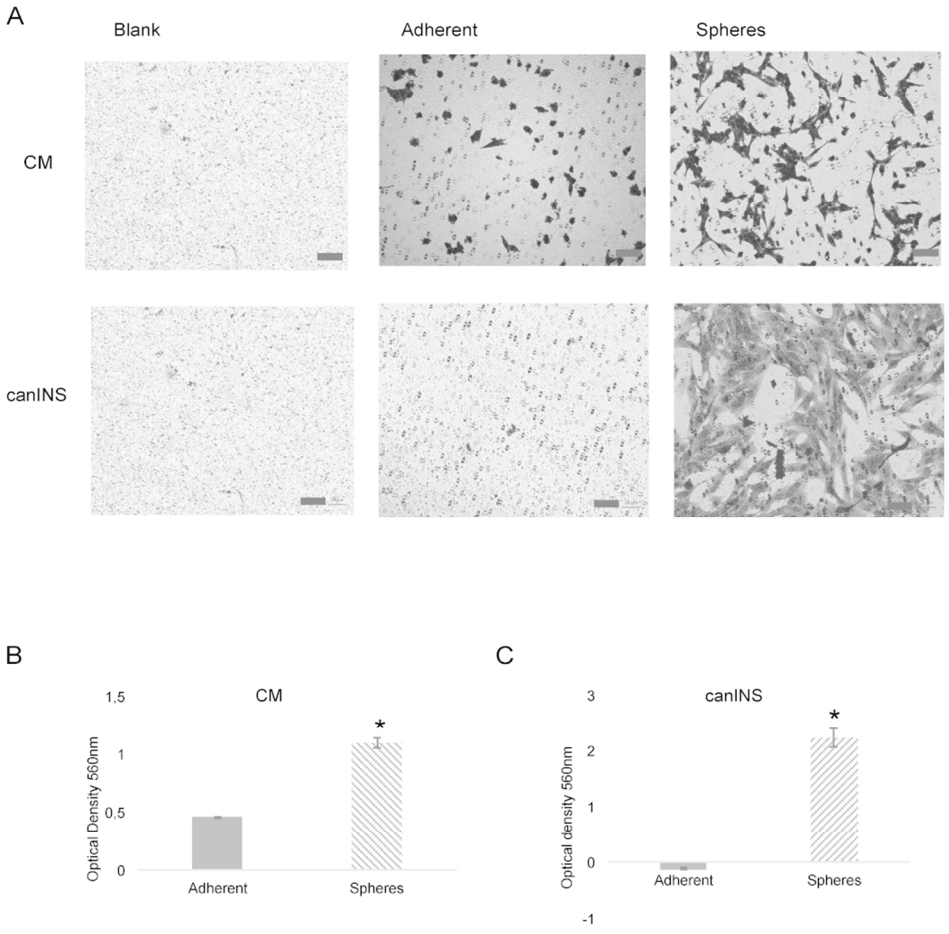

188x177mm (150 x 150 DPI)

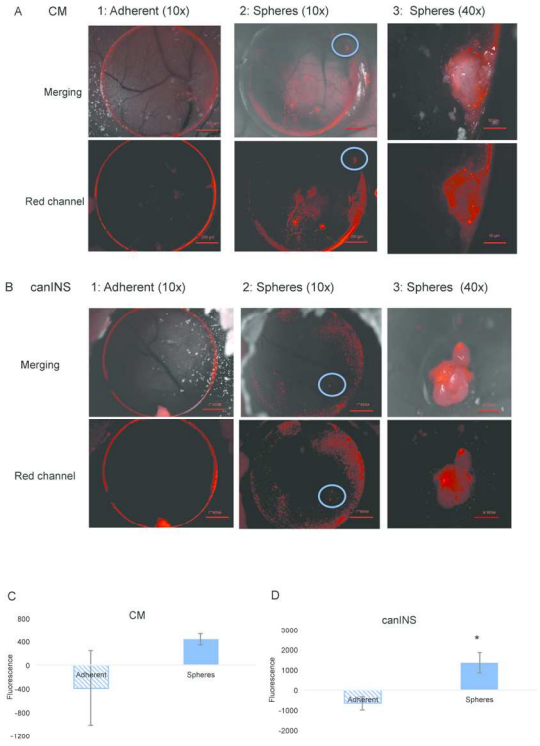

312x296mm (150 x 150 DPI)

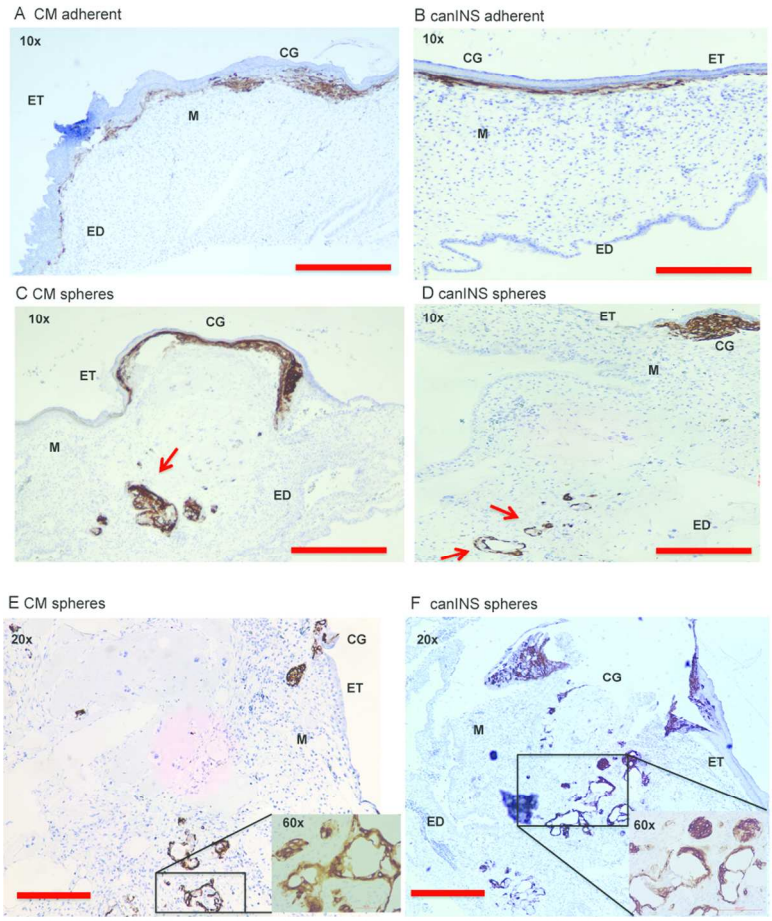

184x260mm (150 x 150 DPI)

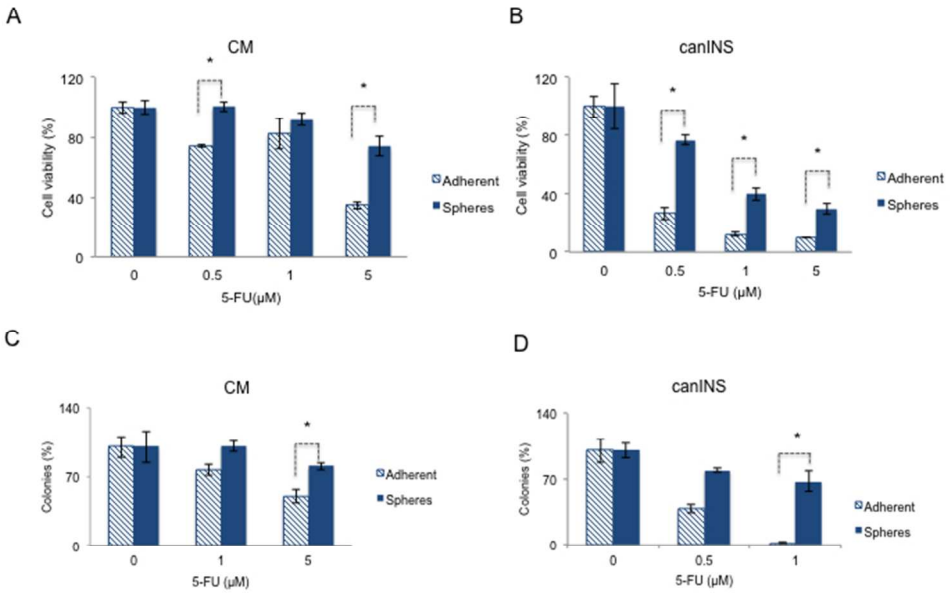

254x190mm (72 x 72 DPI)

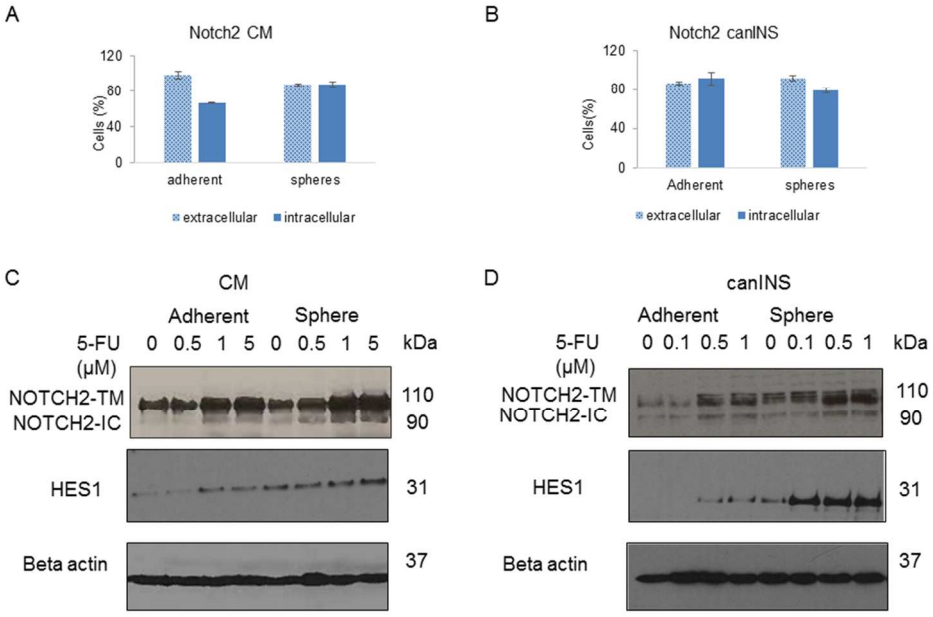

254x190mm (96 x 96 DPI)

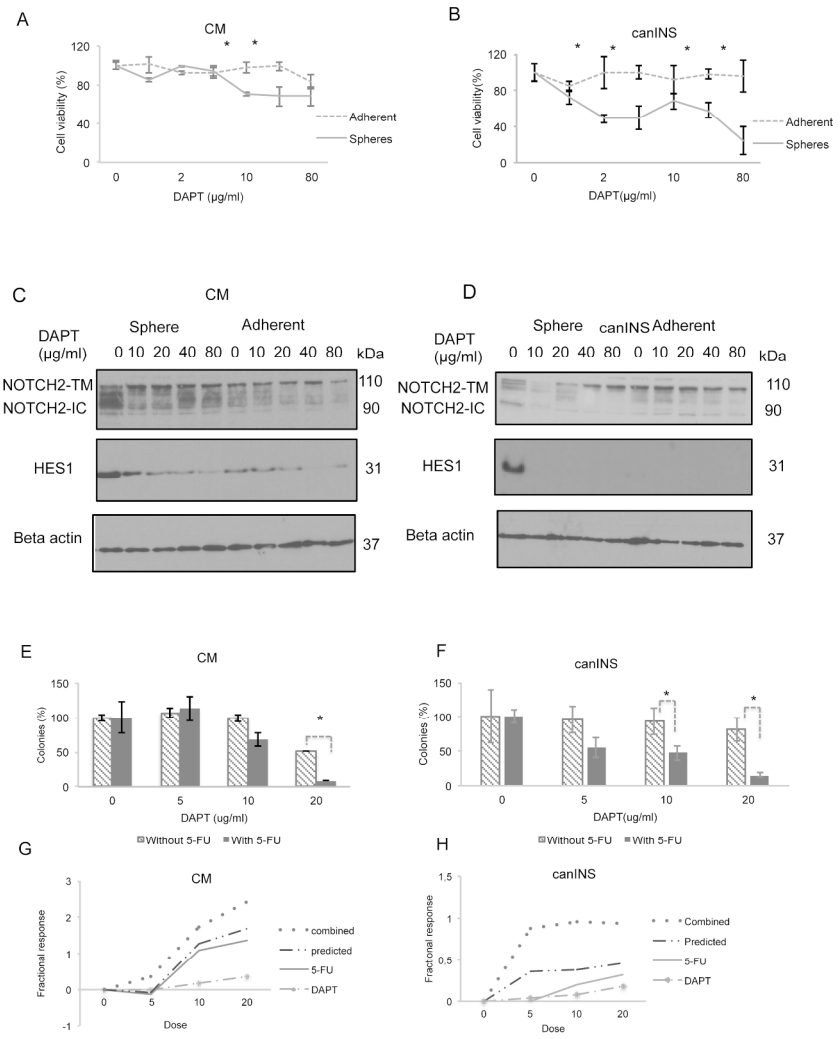

183x254mm (300 x 300 DPI)

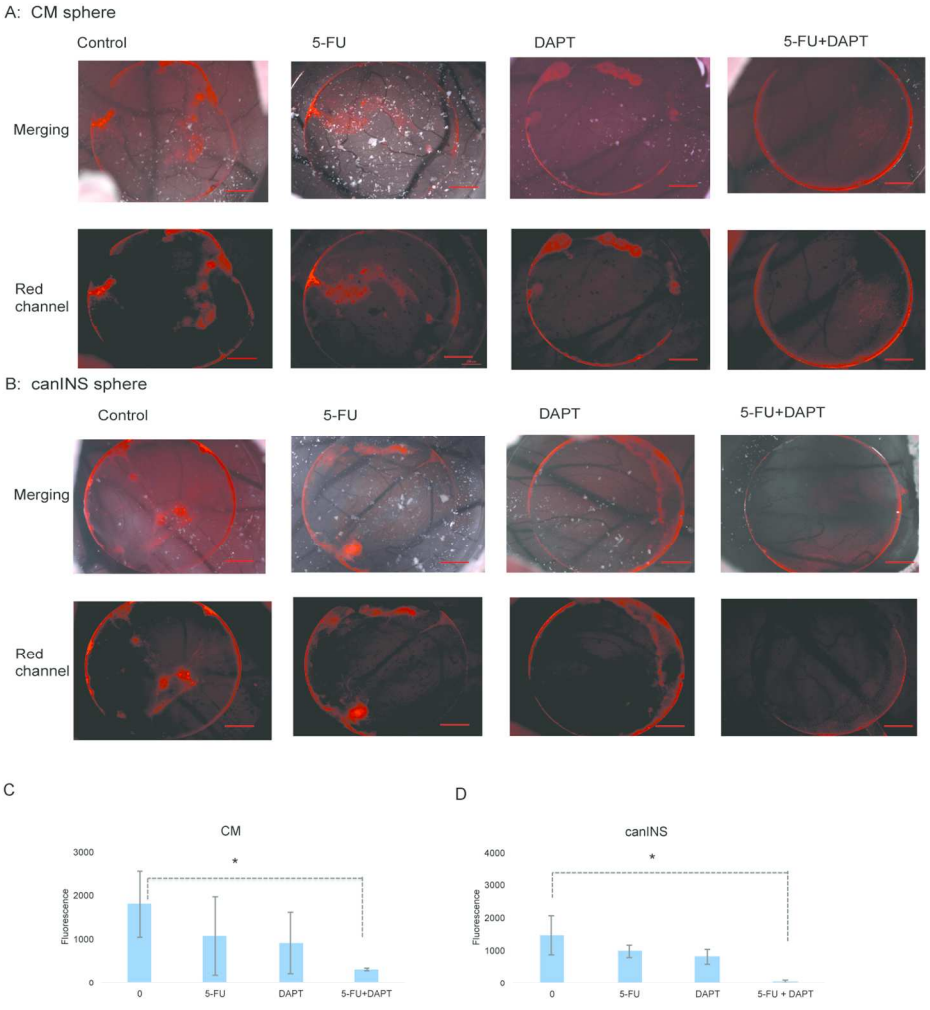

239x303mm (150 x 150 DPI)